DOI 10.47176/sjfst.8.2.1

Original Article

SRPH

SJFST, 2026; 8(2): 1-9

Development of Eugenol-Embedded Chitosan-Mesoporous Silica Nanoparticle Antimicrobial Coatings for Biofilm Control on Medical Devices

Mahfam Alijaniha[1,*] Mahdin Alijaniha[2] Mahdi Mirzaalimohammadi[3]

[1]Zanjan University of Medical Sciences, Iran
[2]Tabriz University of Medical Sciences, Iran
[3]Semnan Azad University, Iran

***Corresponding Author:**
m.gerami@itrc.ac.ir

Received: 15 February, 2026
Revised: 20 April, 2026
Accepted: 09 June, 2026
Published: 25 June, 2026

ABSTRACT

Objective: This study aims to develop an antimicrobial coating using eugenol, an essential oil component, incorporated into chitosan and mesoporous silica nanoparticles (MSNs) to inhibit biofilm formation on medical devices.
Methods: MSNs were synthesized using the Stöber method [1], loaded with eugenol, and embedded into a crosslinked chitosan coating. The coatings were characterized using techniques such as SEM, FTIR, and XPS. Eugenol release was evaluated under different pH conditions. Antimicrobial and antibiofilm activities were tested against Staphylococcus aureus, methicillin-resistant S. aureus (MRSA), and Pseudomonas aeruginosa using growth inhibition assays, Live/Dead staining, and SEM. Biocompatibility was assessed with NIH/3T3 fibroblasts.
Results: The eugenol-loaded coating demonstrated controlled release, with increased release at pH 6 compared to pH 7.4. It significantly reduced planktonic growth and biofilm formation of all tested bacteria, killing >94% of adherent cells. The chitosan coating alone showed limited antimicrobial activity. The eugenol-containing coating was biocompatible in indirect contact but slightly reduced cell metabolic activity in direct contact.
Conclusion: The eugenol-releasing chitosan-MSN coating effectively inhibits biofilm formation and demonstrates potential as an antimicrobial surface for medical devices. Incorporating antimicrobial agents like eugenol is essential for optimal antibiofilm activity. This work provides a foundation for developing chitosan-based coatings with other essential oils or antibiotic alternatives.

Keywords: Antimicrobial coatings, essential oils, biofilm control, eugenol, chitosan, mesoporous silica nanoparticles (MSNs)

Introduction

Biofilms are structured communities of bacteria that adhere to surfaces and produce extracellular polymeric substances (EPS), making them highly resistant to antibiotics and immune responses [2]. These biofilms are a major cause of healthcare-associated infections (HAIs), particularly on medical devices such as catheters, implants, and prosthetics [3]. It is estimated that biofilms account for over 65% of HAIs, leading to increased morbidity, mortality, and healthcare costs [4]. The resistance of biofilms to conventional antibiotics is due to their dense EPS matrix, which limits drug penetration, and their ability to exchange antibiotic-resistant genes through quorum sensing (QS) [5].

Traditional approaches to treating biofilm-related infections often involve the removal of infected devices and extensive debridement, which are costly and traumatic for patients [6]. To address this issue, there is a growing interest in developing antimicrobial surfaces that prevent biofilm formation [7]. One promising strategy is the use of smart coatings that release antimicrobial agents in response to bacterial presence, such as pH changes caused by bacterial metabolism [8]. This approach minimizes unnecessary drug release, reducing the risk of bacterial resistance and cytotoxicity [9]. While many studies have focused on antibiotic-based coatings, there is increasing concern about antibiotic resistance [10].

[DOI: 10.47176/sjfst.8.2.1]

Publisher: Scientific Research Publishing House (SRPH), Shirvan, Iran
http://srpub.org
Email: sjfst@srpub.org

As a result, researchers are exploring alternative antimicrobial agents, such as essential oils (EOs) and their components [11]. EOs are natural compounds extracted from plants and have been shown to possess broad-spectrum antimicrobial, antibiofilm, and anti-QS properties [12]. However, their application in antimicrobial coatings is limited due to their poor water solubility, high volatility, and low stability [13].

This study focuses on eugenol, a major component of clove essential oil, which has demonstrated potent antimicrobial and antibiofilm activity [14]. Eugenol is incorporated into a chitosan matrix, a biocompatible and biodegradable polymer [15], using mesoporous silica nanoparticles (MSN) as a delivery system [16]. The goal is to develop a pH-responsive coating that releases eugenol in the presence of bacterial infections, effectively inhibiting biofilm formation on medical devices [17].

Materials and Methods

Synthesis and Characterization of MSNs

MSNs were synthesized using the Stöber method [1], which involves the hydrolysis and condensation of tetraethyl orthosilicate (TEOS) in the presence of a surfactant. The synthesized MSNs were characterized using dynamic light scattering (DLS) for particle size, Brunauer-Emmett-Teller (BET) analysis for surface area and pore size [18], and scanning electron microscopy (SEM) for morphology [19].

Loading Eugenol into MSNs

Eugenol was loaded into MSNs using a solvent-based adsorption method [20]. MSNs were dispersed in a solution of eugenol in n-hexane, and the mixture was stirred for 24 hours. The encapsulation efficiency was determined by measuring the unloaded eugenol in the supernatant using UV-Vis spectrophotometry [21].

Fabrication of Chitosan Coatings

Chitosan was dissolved in acetic acid and crosslinked with glutaraldehyde (GA) to form a hydrogel matrix [22]. MSNs loaded with eugenol (MSN-EUG) were incorporated into the chitosan solution, and the mixture was drop-casted onto glass substrates to form coatings [23].

Characterization of Coatings

The coatings were characterized using attenuated total reflectance-Fourier transform infrared spectroscopy (ATR-FTIR) to identify chemical bonds [24], X-ray photoelectron spectroscopy (XPS) to analyze surface elemental composition [25], and 3D optical profilometry to measure thickness and roughness [26].

Release Studies

The release of eugenol from the coatings was studied in phosphate-buffered saline (PBS) at pH 6 and 7.4 to simulate acidic and physiological conditions, respectively [27]. The cumulative release was measured using UV-Vis spectrophotometry over 192 hours [28].

Antimicrobial and Antibiofilm Activity

The coatings were tested against Staphylococcus aureus, methicillin-resistant S. aureus (MRSA), and Pseudomonas aeruginosa [29]. Growth inhibition assays were performed to evaluate the effect on planktonic bacteria [30], while Live/Dead staining and confocal laser scanning microscopy (CLSM) were used to assess biofilm formation and bacterial viability [31]. SEM was used to study bacterial morphology and membrane integrity [32].

Biocompatibility

The biocompatibility of the coatings was evaluated using NIH/3T3 mouse fibroblasts [33]. Direct contact assays involved placing the coatings on adherent cells, while indirect contact assays used extracts of the coatings [34]. Cell metabolic activity was measured using the MTT assay [35].

Results and Discussion

Characterization of Mesoporous Silica Nanoparticles (MSNs)

The synthesized MSNs were characterized using various techniques. The Brunauer–Emmett–Teller (BET) analysis revealed a high surface area of 1587.80 m^2/g, with a pore size of 3.30 nm and a pore volume of 1.31 cm^3/g [18]. Dynamic Light Scattering (DLS) measurements indicated an average hydrodynamic diameter of 275 nm while Scanning Electron Microscopy (SEM) showed a particle diameter of 187.0 ± 28.0 nm [19]. Fourier Transform Infrared (FTIR) spectroscopy confirmed the presence of Si–O–Si bonds, indicating the successful synthesis of MSNs [24].

Encapsulation Efficiency of Eugenol in MSNs

Eugenol was encapsulated into MSNs with an efficiency of 74.5 ± 1.4%, corresponding to 1.98 ± 0.042 μL of eugenol per mg of MSNs [20]. The release profile of eugenol from MSNs in PBS showed an initial slow release, peaking at 24 hours with 6.26 ± 1.0% release, followed by a decrease over time [28].

Development and Characterization of Chitosan-Based Coatings

Chitosan coatings crosslinked with glutaraldehyde (GA) were developed, with GA concentrations ranging from 0.5% to 12% [22]. The swelling ratios of the coatings were highest for GA0.5%-CHI and GA1%-CHI, indicating greater hydration and potential for pH-responsive release [27]. The incorporation of eugenol-loaded MSNs (MSN-EUG) into the chitosan matrix resulted in a composite coating (GA0.5%-CHI-MSN-EUG) with increased roughness (Ra = 11.0 ± 1.5 μm) and thickness (88.9 ± 3.8 μm) compared to the pure chitosan coating [26].

Release Kinetics of Eugenol from Composite Coatings

The release of eugenol from GA0.5%-CHI-MSN-EUG and GA1%-CHI-MSN-EUG coatings was evaluated in PBS at pH 6 and 7.4 [27]. The release profile followed a similar pattern to that of MSN-EUG, with an initial low release, peaking at 24 hours (1.28 ± 0.062% at pH 6), and then decreasing.

[DOI: 10.47176/sjfst.8.2.1]

The release was slightly higher at pH 6 compared to pH 7.4, indicating a pH-responsive behavior [28].

Antimicrobial and Antibiofilm Activities

The antimicrobial and antibiofilm activities of the coatings were tested against Staphylococcus aureus (S. aureus), methicillin-resistant S. aureus (MRSA), and Pseudomonas aeruginosa (P. aeruginosa) [29]. The GA0.5%-CHI-MSN-EUG coating significantly reduced the planktonic growth of S. aureus, MRSA, and P. aeruginosa by 99.4%, 94.8%, and 66.6%, respectively [30]. Live/Dead staining and confocal laser scanning microscopy (CLSM) revealed that the eugenol-containing coating significantly reduced bacterial adhesion and increased the percentage of dead cells compared to the control coatings [31]. SEM images confirmed the disruption of bacterial membranes and severe morphological distortions in bacteria exposed to the eugenol-containing coating [32].

Biocompatibility

The biocompatibility of the coatings was assessed using NIH/3T3 mouse fibroblasts [33]. The GA0.5%-CHI and GA0.5%-CHI-MSN coatings showed no cytotoxicity in both direct and indirect contact methods. However, the GA0.5%-CHI-MSN-EUG coating exhibited a 46.7% reduction in cell metabolic activity in direct contact, indicating some cytotoxicity, though it was still less toxic than the 10% DMSO control [35].

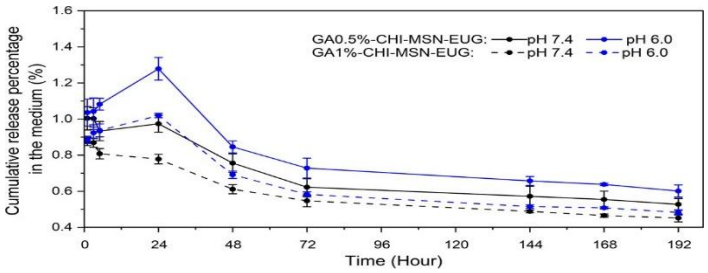

Figure 1. Cumulative release percentage of eugenol from GA0.5% and GA1%-CHI-MSN- EUG coatings in PBS pH 6 and 7.4 at 37oC. Values are expressed as means ± SD (n = 3).

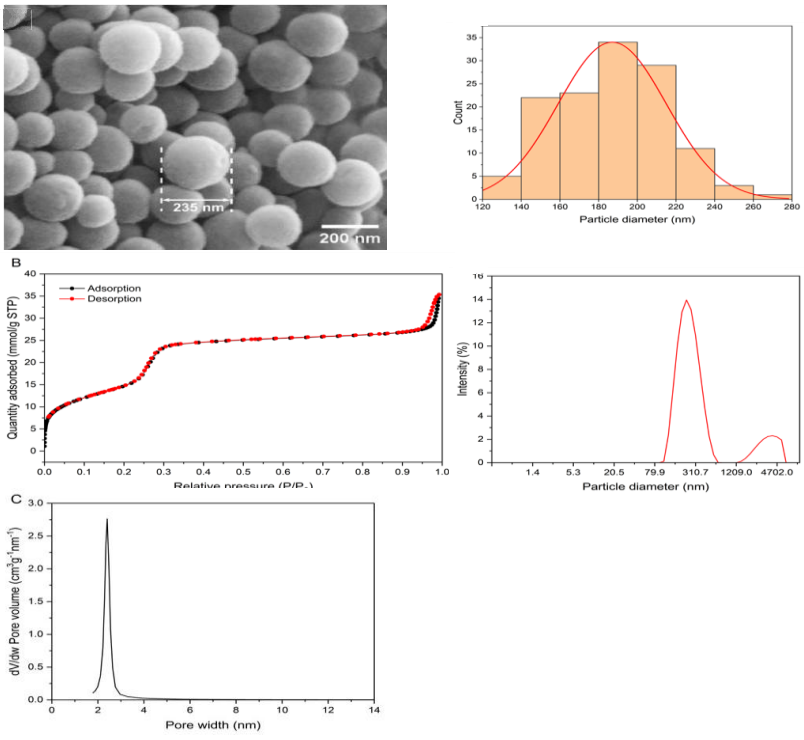

Figure 2. Morphology and pore structure of MSNs. Surface morphology of MSNs observed by SEM (A), N2 adsorption-desorption isotherms at 77 K for MSNs (B) and pore width distribution graph of MSNs (C), particle diameter distribution determined by SEM (n= 128 particles measured over three samples) (D) and DLS (E). Pore widths were estimated using the BJH model applied to the adsorption branch of the isotherm.

[DOI: 10.47176/sjfst.8.2.1]

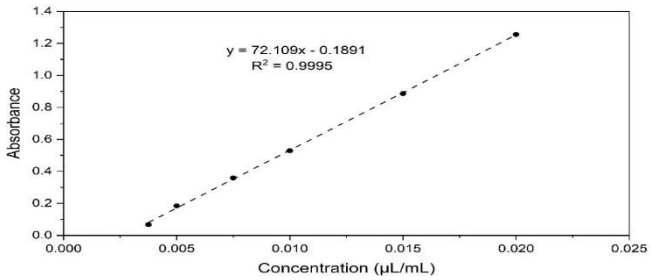

Figure 3. Calibration curve of eugenol in n-hexane

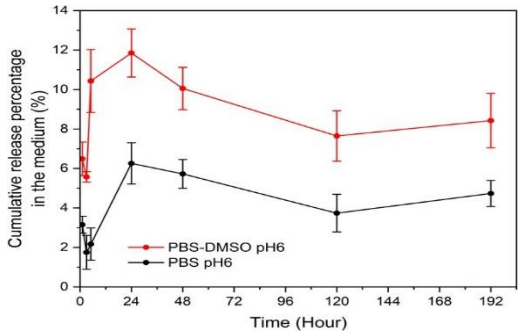

Figure.4. Cumulative release percentage of eugenol from MSNs in PBS pH 6 and PBS– DMSO pH 6 at 37oC. Each data point represents mean ± SD (n = 3).

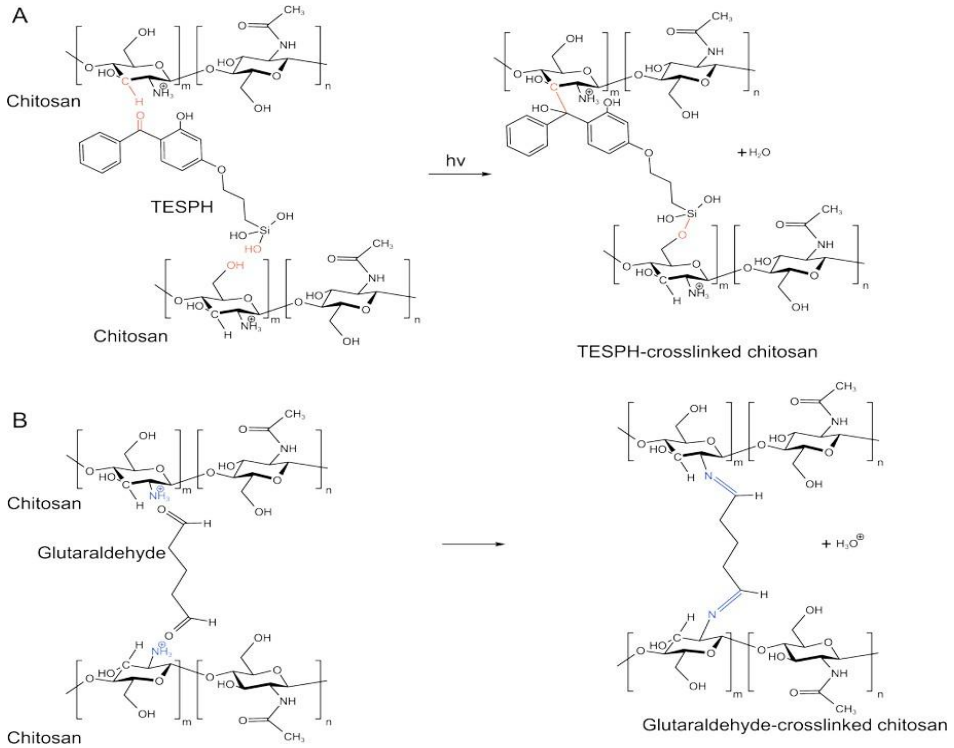

Figure 5. Reaction schemes of chitosan crosslinking by TESPH and glutaraldehyde.

[DOI: 10.47176/sjfst.8.2.1]

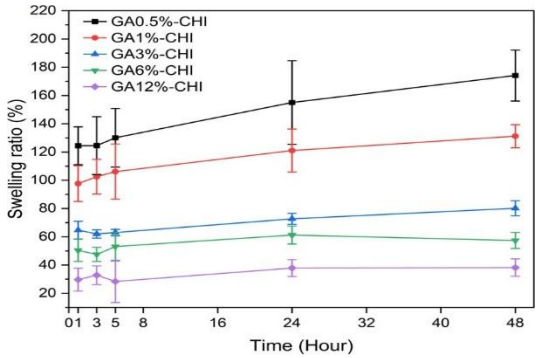

Figure 6. Swelling ratio curve of chitosan coatings crosslinked with different GA concentrations in PBS pH 6 at 37oC over 48 hours. Each data point represents mean ± SD (n= 3).

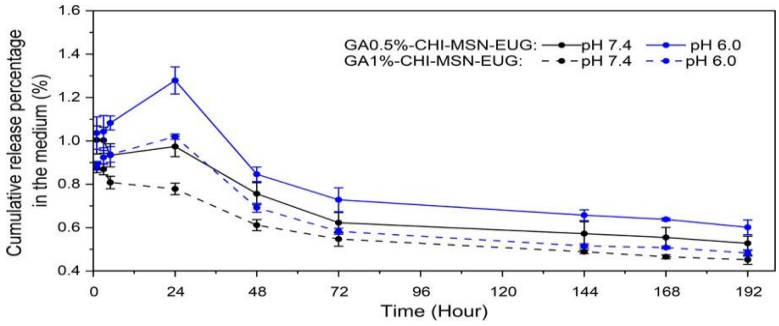

Figure 7. Cumulative release percentage of eugenol from GA0.5% and GA1%-CHI-MSN- EUG coatings in PBS pH 6 and 7.4 at 37oC. Values are expressed as means ± SD (n = 3).

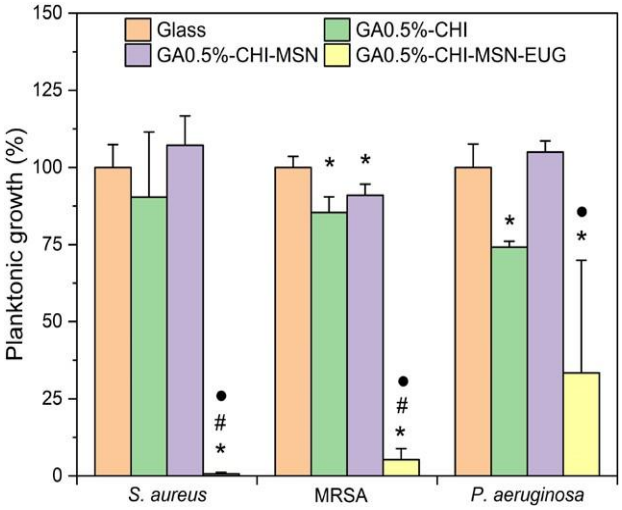

Figure 8. Planktonic growth (%) of *S. aureus*, MRSA, and *P. aeruginosa* after 24 h incubation with different coatings. Values are expressed as mean ± SD (n = 6). A significant difference was defined as *: $p < 0.05$ compared to glass control, #: $p < 0.05$ compared to GA0.5%-CHI, and ●: $p < 0.05$ compared to GA0.5%-CHI-MSN.

[DOI: 10.47176/sjfst.8.2.1]

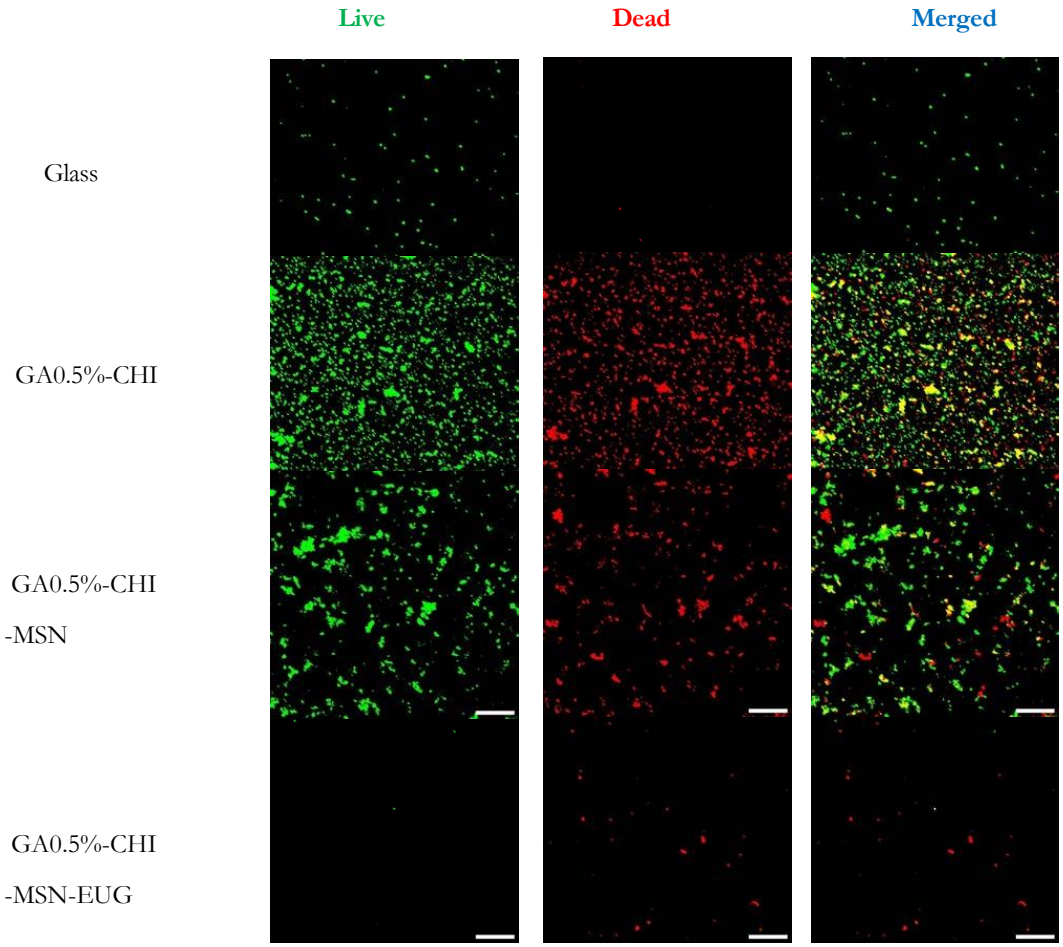

Figure 9. Representative CLSM images of live/dead stained S. aureus on chitosan-based coatings and glass substrate after incubation in the growth medium for 24 h. Scale bar = 40 μm.

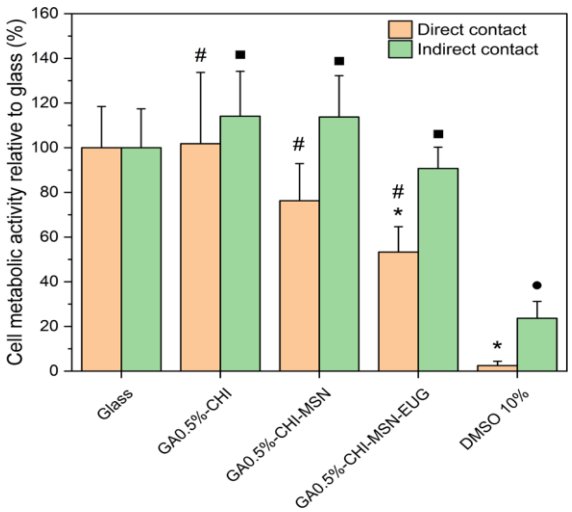

Figure10. The metabolic activity of NIH/3T3 fibroblasts after direct and indirect contact with the coatings relative to glass and DMSO 10% controls. Results are reported as means ± SD (n = 8). The significant difference was defined as * and #: $p < 0.05$ compared to glass and 10% DMSO, respectively in the direct contact method, ● and : $p < 0.05$ compared to glass and 10% DMSO, respectively in the indirect contact method.

[DOI: 10.47176/sjfst.8.2.1]

Table 1. Summary of BET surface area, pore size, and pore volume of MSNs calculated from the N_2 adsorption-desorption isotherm.

Parameter	MSNs
BET surface area[a] (m^2/g)	1587.80
BJH adsorption surface area (m^2/g)	1587.29
BJH desorption surface area (m^2/g)	1618.10
BJH adsorption pore width (nm)	3.30
BJH desorption pore width (nm)	3.27
BJH adsorption pore volume (cm^3/g)	1.31
BJH desorption pore volume (cm^3/g)	1.32

Table 2. Average thickness and roughness (Ra) of chitosan-based coatings.

Coating	Thickness (μm)	Roughness (Ra) (μm)
GA0.5%-CHI	75.3 ± 0.77	0.162 ± 0.030
GA0.5%-CHI-MSN-EUG	88.9 ± 3.8	11.0 ± 1.5

Table 3. Minimum inhibitory concentrations of eugenol against S. aureus, MRSA, and P. aeruginosa.

Bacteria	MIC (μL/mL)	MIC (μg/mL)	MIC (mM)
S. aureus	0.625 ± 0.0	666.9 ± 0.0	4.06 ± 0.0
MRSA	0.833 ± 0.361	888.8 ± 385.2	5.41 ± 2.3
P. aeruginosa	2.5 ± 0.0	2,667.5 ± 0.0	16.24 ± 0.0

Discussion

The development of antimicrobial coatings for medical devices is a critical area of research, particularly in the context of biofilm-associated infections [2]. This study successfully developed a chitosan-based coating embedded with eugenol-loaded mesoporous silica nanoparticles (MSNs) that demonstrated controlled release, significant antimicrobial activity, and biocompatibility [20]. The results highlight the potential of this coating as a pH-responsive antimicrobial surface for medical devices [27].

Eugenol, a major component of clove essential oil, was chosen for its potent antimicrobial and antibiofilm properties [14]. The incorporation of eugenol into MSNs allowed for controlled release, with higher release observed at pH 6 compared to pH 7.4, mimicking the acidic environment of bacterial infections [28]. This pH-responsive behavior is crucial for targeted drug delivery, minimizing unnecessary release and reducing the risk of bacterial resistance [9].

The chitosan matrix provided a biocompatible and biodegradable platform for the MSN-EUG system [15]. Chitosan's positively charged amine groups interact with the negatively charged bacterial membranes, enhancing antimicrobial activity [36-40]. However, crosslinking with glutaraldehyde (GA) reduced the number of free amine groups, which may have limited the intrinsic antimicrobial activity of chitosan [22]. This underscores the importance of incorporating antimicrobial agents like eugenol to enhance the coating's efficacy [14].

The GA0.5%-CHI-MSN-EUG coating demonstrated significant reductions in planktonic growth of Staphylococcus aureus(99.4%), methicillin-resistant S. aureus(MRSA) (94.8%), and Pseudomonas aeruginosa(66.6%) [30].

The coating also reduced biofilm formation and increased the percentage of dead adherent cells, as confirmed by Live/Dead staining and SEM [31]. These results align with previous studies showing that eugenol inhibits biofilm formation at sub-MIC concentrations, likely through membrane disruption and quorum sensing inhibition [14].

Biocompatibility testing revealed that the GA0.5%-CHI-MSN-EUG coating was non-toxic in indirect contact but caused a 46.7% reduction in cell metabolic activity in direct contact [35]. This could be attributed to the high local concentration of eugenol at the coating surface before diffusion into the medium [28].

[DOI: 10.47176/sjfst.8.2.1]

Further optimization of the eugenol loading and release kinetics may improve biocompatibility while maintaining antimicrobial efficacy [27].

Future Directions

1. Optimization of Release Kinetics: Adjusting the crosslinking density and MSN loading to achieve sustained release of eugenol while minimizing cytotoxicity [27].
2. Testing on Medical Devices: Evaluating the coating's performance on real medical devices such as catheters and implants [17].
3. In Vivo Studies: Assessing the coating's efficacy and biocompatibility in animal models to validate its potential for clinical applications [33].
4. Exploration of Other Essential Oils: Investigating the incorporation of other essential oils or antibiotic alternatives to broaden the coating's antimicrobial spectrum [11].

Conclusion

The eugenol-releasing chitosan-MSN coating developed in this study represents a promising strategy for preventing biofilm formation on medical devices. Its pH-responsive release, broad-spectrum antimicrobial activity, and biocompatibility make it a viable alternative to traditional antibiotic-based coatings. This work provides a foundation for further development of chitosan-based coatings with essential oils or other antimicrobial agents for medical applications.

References

1. W. Stöber, A. Fink, and E. Bohn, "Controlled growth of monodisperse silica spheres in the micron size range," Journal of Colloid and Interface Science, vol. 26, no. 1, pp. 62-69, 1968.
2. C. W. Hall and T.-F. Mah, "Molecular mechanisms of biofilm-based antibiotic resistance and tolerance in pathogenic bacteria," FEMS Microbiol. Rev., vol. 41, no. 3, pp. 276-301, 2017.
3. M. Alijaniha, and M. Alijaniha, M. Mirzaalimohammadi. Application of Nanofibers in Drug Delivery, in the Eighth International Conference on Interdisciplinary Studies in Nanotechnology, 2025.
4. J. D. Bryers, Medical biofilms, Biotechnol. Bioeng., vol. 100, no. 1, pp. 1-18, 2008.
5. D. Sharma, L. Misba, and A. U. Khan, "Antibiotics versus biofilm: an emerging battleground in microbial communities," Antimicrob. Resist. Infect. Control, vol. 8, no. 1, p. 76, 2019.
6. S. L. Percival, L. Suleman, C. Vuotto, and G. Donelli, "Healthcare-associated infections, medical devices, and biofilms: risk, tolerance and control," J. Med. Microbiol., vol. 64, no. 4, pp. 323-334, 2015.
7. Y. Cheng, G. Feng, and C. I. Moraru, "Micro- and nanotopography Sensitive Bacterial Attachment Mechanisms: A Review," Front. Microbiol., vol. 10, p. 191, 2019.
8. S. Wu, B. Zhang, Y. Liu, X. Suo, and H. Li, Influence of surface topography on bacterial adhesion: A review (Review), Biointerphases, vol. 13, no. 6, p. 060801, 2018.
9. U. Mahanta, M. Khandelwal, and A. S. Deshpande, Antimicrobial surfaces: a review of synthetic approaches, applicability, and outlook, J. Mater. Sci., vol. 56, no. 32, pp. 17915-17941, 2021.
10. J. A. D. Olmo, L. Ruiz-Rubio, L. Pérez-Alvarez, V. Sáez-Martínez, and J. L. Vilas-Vilela, "Antibacterial coatings for improving the performance of biomaterials," Coatings, vol. 10, no. 2, p. 139, 2020.
11. M. Hassan, M. Alijaniha, S. Jafari, and A. Ghafari, "Physicochemical Properties and Antimicrobial Efficacy of Eugenol Nanoemulsion Formed by Spontaneous Emulsification," Chemical Papers, pp. 1–9, Dec. 2024, Published by Springer International Publishing.
12. P. C. Balaure and A. M. Grumezescu, "Recent advances in surface nanoengineering for biofilm prevention and control. Part i: Molecular basis of biofilm recalcitrance. Passive anti-biofouling nanocoatings," Nanomaterials, vol. 10, no. 6, pp. 1-30, 2020.
13. M. Alijaniha, "Preparation of Eugenol Nanoemulsion by the Spontaneous Method," in 7th International Conference on Interdisciplinary Studies in Nanotechnology, 2023. [Online]. Available: https://civilica.com/doc/2005446.
14. G. Bhagwat, W. O'Connor, I. Grainge, and T. Palanisami, "Understanding the Fundamental Basis for Biofilm Formation on Plastic Surfaces: Role of Conditioning Films," Front. Microbiol., vol. 12, p. 687118, 2021.
15. C. D. Rummel et al., "Conditioning Film and Early Biofilm Succession on Plastic Surfaces," Environ. Sci. Technol., vol. 55, no. 16, pp. 11006-11018, 2021.
16. G. Orazi and G. A. O'Toole, "It Takes a Village": Mechanisms Underlying Antimicrobial Recalcitrance of Polymicrobial Biofilms," J. Bacteriol., vol. 202, no. 1, pp. e00530-19, 2019.
17. Z. Khatoon, C. D. McTiernan, E. J. Suuronen, T. F. Mah, and E. I. Alarcon, "Bacterial biofilm formation on implantable devices and approaches to its treatment and prevention," Heliyon, vol. 4, no. 12, p. e01067, 2018.
18. K. S. W. Sing, "Reporting physisorption data for gas/solid systems with special reference to the determination of surface area and porosity (Recommendations 1984),"
19. J. Wang, G. Wang, Z. Zhang, G. Ouyang, and Z. Hao, "Effects of mesoporous silica particle size and pore structure on the performance of polymer-mesoporous silica mixed matrix membranes," RSC Adv., vol. 11, no. 58, pp. 36577-36586, 2021.
20. M. Bravo Cadena, G. M. Preston, R. A. L. Van der Hoorn, H. E. Townley, and I. P. Thompson, "Species-specific antimicrobial activity of essential oils and enhancement by encapsulation in mesoporous silica nanoparticles," Ind. Crops Prod., vol. 122, pp. 582-590, 2018.

[DOI: 10.47176/sjfst.8.2.1]

21. X. Hu, Y. Wang, and B. Peng, "Chitosan-Capped Mesoporous Silica Nanoparticles as pH-Responsive Nanocarriers for Controlled Drug Release," Chem. Asian J., vol. 9, no. 1, pp. 319-327, 2014.
22. K. AbouAitah et al., "Novel delivery system with a dual–trigger release of savory essential oil by mesoporous silica nanospheres and its possible targets in leukemia cancer cells: in vitro study," Cancer Nanotechnol., vol. 14, no. 1, p. 3, 2023.
23. A. Jobdeedamrong, R. Jenjob, and D. Crespy, "Encapsulation and Release of Essential Oils in Functional Silica Nanocontainers," Langmuir, vol. 34, no. 44, pp. 13235-13243, 2018.
24. Y. Liu, Z. Cai, L. Sheng, M. Ma, Q. Xu, and Y. Jin, "Structure-property of crosslinked chitosan/silica composite films modified by genipin and glutaraldehyde under alkaline conditions," Carbohydr. Polym., vol. 215, pp. 348-357, 2019.
25. M. Slattery, J. Amini, and R. Hallaj, "Antifungal activity of the lemongrass and clove oil encapsulated in mesoporous silica nanoparticles against wheat's take-all disease," Pestic. Biochem. Physiol., p. 104696, 2020.
26. M. Hoyos-Nogues, F. Velasco, M. P. Ginebra, J. M. Manero, F. J. Gil, and C. Mas-Moruno, "Regenerating Bone via Multifunctional Coatings: The Blending of Cell Integration and Bacterial Inhibition Properties on the surface of Biomaterials," ACS Appl. Mater. Interfaces, vol. 9, no. 26, pp. 21618-21630, 2017.
27. A. Hernández-Rangel et al., Fabrication and in vitro behavior of dual-function chitosan/silver nanocomposites for potential wound dressing applications, Mater. Sci. Eng. C, vol. 94, pp. 750-765, 2019.
28. T. Y. Liao, C. D. Easton, H. Thissen, and W. B. Tsai, "Aminomalononitrile-Assisted Multifunctional Antibacterial Coatings," ACS Biomater. Sci. Eng., vol. 6, no. 6, pp. 3349-3360, 2020.
29. K. Punjabi et al., "Biopolymer Coating Imparts Sustainable Self-Disinfecting and Antimicrobial Properties to Fabric: Translated to Protective Gears for the Pandemic and Beyond," ACS Biomater. Sci. Eng., vol. 9, no. 2, pp. 1116-1131, 2023.
30. Y. Huang, N. Dan, W. Dan, and W. Zhao, "Reinforcement of Polycaprolactone/Chitosan with Nanoclay and Controlled Release of Curcumin for Wound Dressing," ACS Omega, vol. 4, no. 27, pp. 22292-22301, 2019.
31. M. Li, D. Mitra, E. T. Kang, T. Lau, E. Chiong, and K. G. Neoh, "Thiol-ol Chemistry for Grafting of Natural Polymers to Form Highly Stable and Efficacious Antibacterial Coatings," ACS Appl. Mater. Interfaces, vol. 9, no. 2, pp. 1847-1857, 2017.
32. D. Mitra, M. Li, R. Wang, Z. Tang, E.-T. Kang, and K. G. Neoh, "Scalable Aqueous-Based Process for Coating Polymer and Metal Substrates with Stable Quaternized Chitosan Antibacterial Coatings," Ind. Eng. Chem. Res., vol. 55, no. 36, pp. 9603-9613, 2016.
33. H. Wu, Y. Xiao, Y. Guo, S. Miao, Q. Chen, and Z. Chen, "Functionalization of SBA-15 mesoporous materials with 2-acetylthiophene for adsorption of Cr(III) ions," Microporous Mesoporous Mater., vol. 292, p. 109754, 2020.
34. M. Tomozawa, J. W. Hong, and S. R. Ryu, "Infrared (IR) investigation of the structural changes of silica glasses with fictive temperature," J. Non-Cryst. Solids, vol. 351, no. 12-13, pp. 1054-1060, 2005.
35. C. O. Metin, L. W. Lake, C. R. Miranda, and Q. P. Nguyen, "Stability of aqueous silica nanoparticle dispersions," J. Nanopart. Res., vol. 13, no. 2, pp. 839-850, 2010.
36. A. F. A. Rahman et al., "Strategies for introducing titania onto mesostructured silica nanoparticles targeting the enhanced photocatalytic activity of visible-light-responsive Ti-MSN catalysts," J. Clean. Prod., vol. 143, pp. 948-959, 2017.
37. J. A. Schott, C.-L. Do-Thanh, W. Shan, N. G. Puskar, S. Dai, and S. M. Mahurin, "FTIR investigation of the interfacial properties and mechanisms of CO2 sorption in porous ionic liquids," Green Chem. Eng., vol. 2, no. 4, pp. 392-401, 2021.
38. P. Vukosav, L. Pašalić, D. Bakarić, D. Domazet Jurašin, and T. Mišić Radić, "Interaction of Silica Nanoparticles with Microalgal Extracellular Polymers," Water, vol. 15, no. 3, 2023.
39. F. Rancan et al., "Skin Penetration and Cellular Uptake of Amorphous Silica Nanoparticles with Variable Size, Surface Functionalization, and Colloidal Stability," ACS Nano, vol. 6, no. 8, pp. 6829-6842, 2012.
40. N. C. Bell, C. Minelli, J. Tompkins, M. M. Stevens, and A. G. Shard, "Emerging Techniques for Submicrometer Particle Sizing Applied to Stöber Silica," Langmuir, vol. 28, no. 29, pp. 10860-10872, 2012.

SJFST

Citation: Alijaniha M, Alijaniha M, Mirzaalimohammadi M. Development of Eugenol-Embedded Chitosan-Mesoporous Silica Nanoparticle Antimicrobial Coatings for Biofilm Control on Medical Devices. SJFST, 2026; 8(2): 1-9.

https://doi.org/10.47176/sjfst.8.2.1

[DOI: 10.47176/sjfst.8.2.1]